

Influences of dynamical disruptions on the evolution of pulsars in globular clusters

Kwangmin Oh,¹ C. Y. Hui,^{2*} Jongsuk Hong,^{3†} J. Takata,⁴ A. K. H. Kong,⁵ Pak-Hin Thomas Tam,⁶

Kwan-Lok Li,⁷ and K. S. Cheng⁸

¹*Department of Space Science and Geology, Chungnam National University, Daejeon 34134, Korea*

²*Department of Astronomy and Space Science, Chungnam National University, Daejeon 34134, Korea*

³*Korea Astronomy and Space Science Institute, Daejeon 34055, Republic of Korea*

⁴*Department of Astronomy, School of Physics, Huazhong University of Science and Technology, Wuhan 430074, People's Republic of China*

⁵*Institute of Astronomy, National Tsing Hua University, Hsinchu 30013, Taiwan*

⁶*School of Physics and Astronomy, Sun Yat-sen University, Guangzhou 510275, People's Republic of China*

⁷*Department of Physics, National Cheng Kung University, 701401 Tainan, Taiwan*

⁸*Department of Physics, The University of Hong Kong, Pokfulam Road, 999077, Hong Kong*

10 August 2023

ABSTRACT

By comparing the physical properties of pulsars hosted by core-collapsed (CCed) and non-core-collapsed (Non-CCed) globular clusters (GCs), we find that pulsars in CCed GCs rotate significantly slower than their counterparts in Non-CCed GCs. Additionally, radio luminosities at 1.4 GHz in CCed GCs are higher. These findings are consistent with the scenario that dynamical interactions in GCs can interrupt angular momentum transfer processes and surface magnetic field decay during the recycling phase. Our results suggest that such effects in CCed GCs are stronger due to more frequent disruptions of compact binaries. This is further supported by the observation that both estimated disruption rates and the fraction of isolated pulsars are predominantly higher in CCed GCs.

Key words: stars: binaries: general — stars: pulsars: general — globular clusters: general

1 INTRODUCTION

Millisecond pulsars (MSPs) are characterized by fast rotations with rotational periods P_{rot} typically shorter than a few tens of milliseconds and relatively weak surface magnetic fields $B_s \lesssim 10^9$ G (Manchester et al. 2005; Hui & Li 2019). In order to achieve such fast rotation, MSPs are generally believed to have gone through an accretion phase, during which neutron stars gain angular momentum transferred from their companion stars (Alpar et al. 1982; Radhakrishnan & Srinivasan 1982; Fabian et al. 1983). This is commonly referred to as the recycling process. During recycling, mass accretion on the neutron star surface can potentially lead to magnetic field decay, as shown in (Cumming et al. 2004), which might account for the weak dipolar field strength inferred from observations.

MSPs can be further separated into two subgroups according to their locations: those residing in globular clusters (GCs) and those in the Galactic field (GF). Owing to the high stellar densities in GCs, the formation of MSPs inside a cluster can be influenced by intracluster dynamical processes (cf. Sigurdsson & Phinney 1995; Ivanova et al. 2008; Hui et al. 2010; Ye et al. 2019). While primary encounter interactions, such as tidal capture or direct collision with a giant, can facilitate binary formation (Fabian et al. 1975; Press & Teukolsky 1977; Lee & Ostriker 1986; Lombardi et al. 2006; Fregeau & Rasio

2007; Ye et al. 2022), subsequent encounters (referred to as secondary encounters hereafter) can play a role in disrupting binaries (Verbunt & Freire 2014a).

Many studies have shown that dynamical interactions in GCs can lead to an increase in MSP population in comparison with the GF MSPs which rely on binary evolution alone (e.g. Ye et al. 2019; Hui et al. 2010; Ivanova et al. 2008). This is consistent with the well-known fact that the formation rate per unit mass of low-mass X-ray binaries (LMXBs), which are the progenitors of MSPs, is orders of magnitude larger in GCs than in GF (Katz 1975; Clark 1975). Although many more LMXBs can be assembled in GCs, the mass-transferring processes can be interrupted by the subsequent encounters (Verbunt & Freire 2014b). Such intricate dynamics could potentially lead to differences in the properties of MSPs in GCs compared to those in GF.

The sample sizes of the currently known populations of MSPs in GF and GCs are comparable, which allows a reasonable comparison of the properties between these two populations. In a recent study, Lee et al. (2023) performed a systematic comparison of rotational, orbital, and X-ray properties of MSPs in GCs and GF. They found that MSPs in GCs generally rotate slower than those in the GF. There is also an indication that the surface magnetic field of GC MSPs is stronger than those in the GF. These findings are consistent with the scenario that the recycling processes of GC MSPs were interrupted by secondary encounters, leading to shortened epochs for both angular momentum transfer and possible magnetic field decay.

* Corresponding author E-mail: huichungyue@gmail.com

† Corresponding author E-mail: jshong@kasi.re.kr

Based on the photometric concentrations, GCs can be classified into core-collapsed (CCed) and non-core-collapsed (Non-CCed) (Harris 1996, 2010 edition). A core collapse in a GC is likely a result of gravothermal instability (cf. Lynden-Bell & Wood 1968), which can significantly affect the kinematic properties.

While the number of X-ray sources in GCs generally correlates with the primary encounter rate Γ^1 (Pooley et al. 2003), Bahramian et al. (2013) found that CCed GCs have fewer X-ray sources than Non-CCed GCs for the same value of Γ (see Figure 9 in Bahramian et al. (2013)). This might indicate the dynamical status of CCed GCs is different from that of Non-CCed GCs, which can leave an imprint on the evolution of compact binaries. Therefore, it is reasonable to speculate that the properties of GC MSPs may be further diversified between CCed and Non-CCed GCs.

Motivated by the aforementioned findings, we aim to explore potential differences in the properties of pulsars within CCed and Non-CCed GCs by conducting a statistical analysis of selected parameters. In Section 2, we describe our procedure for preparing the data for analysis. The results of statistical analysis are given in Section 3 and their implications will be discussed in Section 4.

2 DATA PREPARATION

First, we have selected a sample of 280 pulsars from 38 different GCs from the Australia Telescope National Facility (ATNF) Pulsar Catalogue (Manchester et al. 2005, ver. 1.70). In this work, we only collected the following parameters from the Catalogue: rotational period P_{rot} , orbital period P_b , radio luminosity in L-band $L_{1.4\text{GHz}}$. On the other hand, we have adopted the X-ray luminosities L_x (0.3–8 keV) of 56 X-ray emitting MSPs from Table 2 in Lee et al. (2023).

Observationally, it is a common practice to classify whether a GC is CCed or Non-CCed based on its surface brightness profile (e.g. Trager et al. 1995; Harris 1996; Rivera Sandoval et al. 2018). Owing to the increased stellar density towards the cluster centre, a GC is defined as CCed if its surface brightness profile exhibits a power law until the limit of observational resolution (Rivera Sandoval et al. 2018; Trager et al. 1995). On the other hand, Non-CCed GCs typically exhibit a flattened profile towards their centres and follow a King profile (Trager et al. 1995; King 1966).

In Section 3.1, we adopted the classifications given by Harris (1996, 2010 version) in determining whether a GC is CCed or Non-CCed. Using these labels, we divided our samples accordingly and compared their properties.

3 STATISTICAL ANALYSIS & RESULTS

3.1 Core-Collapsed GCs versus Non-Core-Collapsed GCs

We conducted a detailed statistical analysis to compare the aforementioned selected properties of pulsars in CCed and Non-CCed GCs. For each population, we first constructed the unbinned empirical cumulative distribution function (eCDF) of the parameters which are shown in Figure 1. By visual inspection, these properties appear to be different between these two populations. To quantify the possible difference, we used a two-sample Anderson-Darling (A-D) test to investigate whether such differences are significant. In this work, we consider the difference between two eCDFs to be significant if the

¹ $\Gamma \propto \rho_c^{1.5} r_c^2$, where ρ_c and r_c are the density and radius of the cluster core respectively.

p -values inferred from A-D test is < 0.05 . The results of the A-D test are summarized in Table 1.

We found that the distributions of P_{rot} and $L_{1.4\text{GHz}}$ from CCed GCs and Non-CCed GCs are significantly different. The corresponding p -values inferred from A-D test are found to be 0.003 and 0.014 respectively. From the distributions of P_{rot} as shown in the upper-right panel of Figure 1, one can see that the pulsars in CCed GCs generally rotate slower than those in Non-CCed GCs. The median of P_{rot} in CCed and Non-CCed populations are 5.24 ms and 4.45 ms respectively.

For $L_{1.4\text{GHz}}$, the distributions of these two groups of GC pulsars are obviously different (lower-left panel of Figure 1). It is very clear that the pulsars in the CCed GCs are more powerful radio emitters. The median of $L_{1.4\text{GHz}}$ in CCed and Non-CCed are found to be 4.29 mJy kpc² and 1.4 mJy kpc² respectively.

Figure 1 suggests that P_b of the pulsars in CCed GCs are shorter, indicating that they have tighter orbits compared to those in Non-CCed GCs. This finding is consistent with our understanding that pulsars with longer orbital periods in CCed GCs are more likely to have been disrupted by dynamical interactions. However, the p -value obtained from the A-D test is 0.24, which falls short of our pre-defined criterion for claiming a significant difference between the two groups. This result may be due to the small sample size.

While Lee et al. (2023) have compared the MSP properties between the GF and GC populations, and identified differences between these them, they did not separately compare GF MSPs with those in CCed GCs and Non-CCed GCs. To complement the analysis conducted by Lee et al. (2023) as well as our aforementioned investigations, we have further compared MSP properties among the populations in the GF, CCed GCs, and Non-CCed GCs.

In comparing with the MSP properties in the GF, we have followed the same selection criterion as in Lee et al. (2023), by selecting pulsars with $P_{\text{rot}} < 20$ ms in all three populations (i.e. GF, CCed GCs and Non-CCed GCs). This procedure can avoid including non-recycled GF pulsars in this part of the analysis. The eCDFs of P_{rot} , P_b , $L_{1.4\text{GHz}}$, and L_x are shown in Figure 2. The results of the A-D tests are summarized in Table 1.

From the distribution of P_{rot} , it is obvious that the rotation of MSPs in the GF is significantly faster than those in CCed and Non-CCed GCs. Moreover, we can see that the difference between CCed GCs and GF is larger than that between Non-CCed GCs and GF. We also find that the P_b of GF MSPs is significantly longer than those in GCs, regardless of whether they are CCed or Non-CCed. All these findings align with the scenario suggested by Lee et al. (2023), which posits that intracluster dynamics have resulted in the formation of more tightly-bound binaries and the interruptions of the recycling process.

For comparing the distributions of luminosities between GF and GC MSPs in X-ray and radio, we found differences that are statistically acceptable (see Table 1). However, given the current sample, it is difficult to rule out the possibility that such differences have resulted from the observational bias between GF and GCs (see the discussion in Section 4).

Since P_{rot} and $L_{1.4\text{GHz}}$ of the MSPs in CCed GCs are found to be significantly different from those in Non-CCed GCs and the GF, we have further examined their distributions by computing the kernel density estimates (KDEs). The results are shown in Figure 3. In the panel of P_{rot} , it clearly shows that the peaks of density distributions systematically shifted towards the larger value from the GF (which lacks dynamical interactions) to the CCed GCs (which have the largest disruption rates among three populations; see Table 2). The peaks for the KDEs of P_{rot} for GF, Non-CCed GCs, and CCed

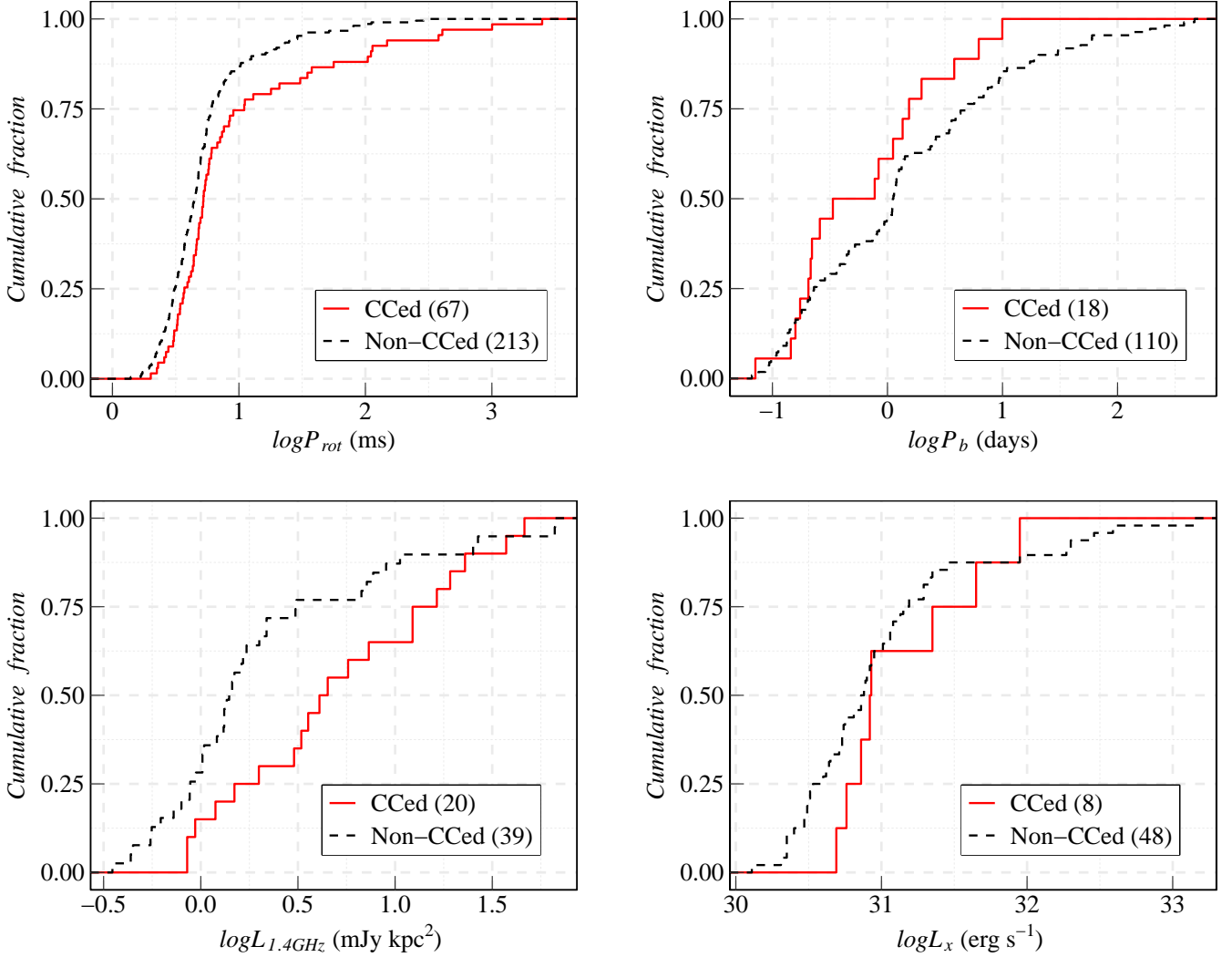


Figure 1. Comparisons of eCDFs of the selected pulsar properties between CCed GCs and Non-CCed GCs. The bracketed numbers in the legends show the corresponding sample sizes.

GCs are 3.6 ms, 4.6 ms, and 5.0 ms respectively. For $L_{1.4\text{GHz}}$, the KDEs of GF and CCed GC populations peaked at 1.8 mJy kpc² and 2.8 mJy kpc² respectively. In the case of Non-CCed GC MSPs, it is interesting to note that there appear to have two peaks in its $L_{1.4\text{GHz}}$ KDE which is located at 1.3 mJy kpc² and 8.0 mJy kpc². However, there are only 7 Non-CCed GC MSPs ≥ 3 mJy kpc² in the current sample which does not allow us to determine whether such multimodal distributions are genuine or simply a fluctuation due to the small sample.

Verbunt & Freire (2014a) have compared the fraction of isolated pulsars in GCs with the corresponding disruption rate $\gamma \propto \rho_c^{0.5} r_c^{-1}$, where ρ_c and r_c represent the central density and core radius, respectively (cf. Tab. 1 in Verbunt & Freire 2014a). In their work, they considered a sample of only 14 GCs. Since our sample is now almost three times larger, it is legitimate to revisit this comparison. For computing γ , we adopted ρ_0 and r_c from Harris (1996, 2010 edition). In Table 2, we compare the numbers of isolated pulsars N_s and binary pulsars N_b in 37 GCs with their corresponding γ . GLIMPSE01 is excluded in this part of the analysis because we cannot find its structural parameters in the literature.

We proceeded to examine if there is any correlation between the

fraction of isolated pulsars $f_s = N_s / (N_s + N_b)$ and γ with the non-parametric Spearman’s rank test, which yields a p -value of 0.014. This indicates the correlation between these two quantities is significant. This prompts us to perform a regression analysis to obtain an empirical relation between f_s and γ . However, in view of the small statistics of pulsar population in most GCs, we notice that the f_s is very sensitive to N_s and N_b . In particular, many of the GCs have $f_s = 0$ (Table 2).

To address this issue, we found that Laplace smoothing is a well-established technique in handling categorical data with a small sample size (e.g. Manning et al. 2008; Gelman et al. 2013). By adding a smoothing parameter α to the observed counts, the method can stabilize the estimates and avoid zero empirical probabilities. With Laplace smoothing, we obtained the smoothed estimate of f_s as $\hat{f}_s = \frac{N_s + \alpha}{N_s + N_b + 2\alpha}$ with α taken to be 1.

In Figure 4, we show the scatter plot between \hat{f}_s and $\log \gamma$ of our sample. It is obvious that the disruption rates of CCed GCs are generally larger than those of Non-CCed GCs. Furthermore, GCs with $\hat{f}_s \geq 0.5$ are predominantly CCed GCs with γ more than ten times larger than the conventional reference level in M4. These findings are fully consistent with the results reported by Verbunt & Freire

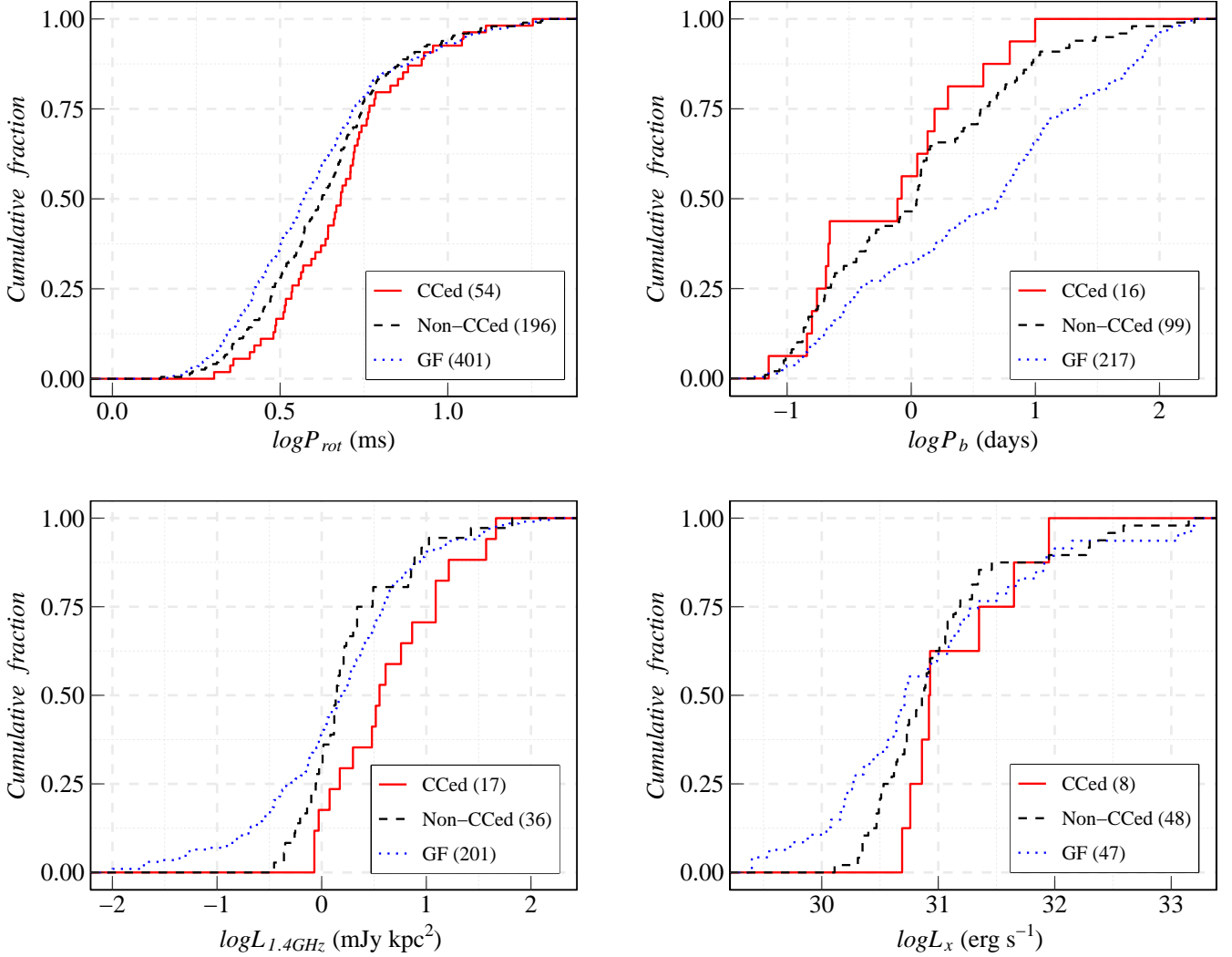


Figure 2. Comparisons of eCDFs of the selected pulsar properties among CCed GCs, Non-CCed GCs, and GF. The bracketed numbers in the legends show the corresponding sample sizes.

	CCed vs non-CCed ¹	CCed vs GF ²	non-CCed vs GF ²	GCs vs GF ³
P_{rot}	0.003	0.002	0.023	0.001
P_b	0.242	0.001	9×10^{-5}	10^{-7}
$L_{1.4\text{GHz}}$	0.014	0.001	0.094	0.041
L_x	0.315	0.137	0.078	0.030

Table 1. Null hypothesis probabilities of A-D test for comparing P_{rot} , P_b , $L_{1.4\text{GHz}}$ and L_x among CCed GCs, Non-CCed GCs and GF.

¹ c.f. Figure 1.

² c.f. Figure 2.

³ GCs = CCed + Non-CCed

(2014a). By fitting a linear model $\hat{f}_s = a \log \gamma + b$ to the data with each GC weighted by the numbers of detected pulsars, we found the best-fit parameters of $a = 0.12 \pm 0.05$ and $b = 0.38 \pm 0.05$ (1σ uncertainties) for this empirical relation. To test whether the result of linear regression is sensitive to the adopted smoothing parameter, we repeated the analysis by varying α from 2 to 5. We found that the results obtained from different α values all lie within the 95% confidence band shown in Figure 4 for the case of $\alpha = 1$.

3.2 Alternative Classification by Unsupervised Clustering

While the aforementioned analyses show that P_{rot} and $L_{1.4\text{GHz}}$ of the MSPs in CCed GCs and Non-CCed GCs are significantly different, the possible ambiguity in the conventional CCed/Non-CCed classification can hamper the robustness of this conclusion. As we have mentioned in Section 2, such classification is determined by the structure of their brightness profiles. In case the central part of GC is poorly resolved, the CCed/Non-CCed classifications are subjected to uncertainties.

This concern is reflected by the central concentration parameters c given in Harris (1996, 2010 version), which is defined as the logarithm of the ratio between tidal radius r_t and core radius r_c . c is deduced from surface brightness profile fitting (Trager et al. 1995; King 1966). For most of the CCed GCs, no reasonable fit can be obtained and an upper bound of $c = 2.5$ is placed instead (cf. Trager et al. 1995; Harris 1996). While c can provide a simple parameter for characterizing the structure, we realize that our sample spans the ranges of $c = 0.79 - 2.07$ and $c = 1.63 - 2.5$ for Non-CCed and CCed GCs, respectively. Such heavily-overlapped ranges of c indicate the CCed/Non-CCed classification in Harris (1996, 2010 version) is not without ambiguity.

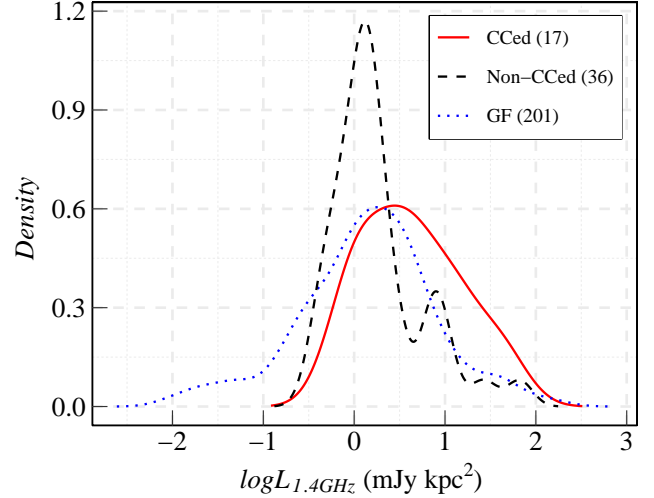
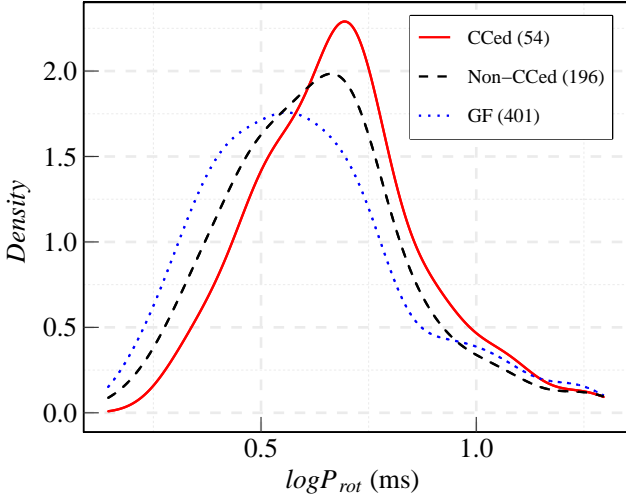


Figure 3. Kernel density estimates for the distributions of $\log P_{\text{rot}}$ and $\log L_{1.4\text{GHz}}$ of MSPs in CCed GCs, Non-CCed GCs, and the GF.

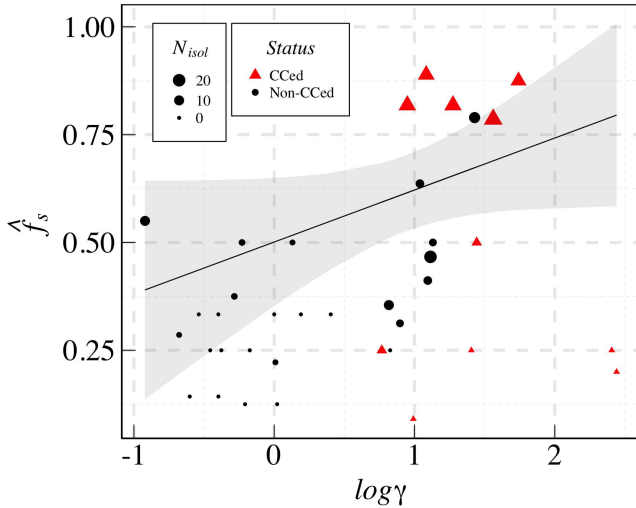


Figure 4. Relation between the fraction of isolated pulsars estimated by Laplace smoothing \hat{f}_s and the disruption rate $\log \gamma$. The symbol sizes scales with the actual number of observed isolated pulsars. The straight line represents the best-fit linear model with 95% confidence band illustrated by the shaded region.

On the other hand, the disruption rates γ in Table 2 might provide a more quantitative measure of the dynamical status of a GC (Verbunt & Freire 2014b). For example, in Figure 4, we have seen that the fraction of isolated pulsars f_s is generally correlated with γ , though the spread of the data from the best-fit linear model is rather wide.

Individually, the parameters γ and c might not allow an unambiguous classification of GCs. This motivates us to examine whether the classification can be improved by combining both parameters.

For deriving the classification rules in the plane spanned by γ and c , we employed the Gaussian Mixture Model (GMM) algorithm. GMM is a probabilistic model with an assumption that the data originated from a mixture of finite numbers of Gaussian components. We have considered a set of models with the number of mixture components ranging from 1 to 9. We utilized the CRAN `McLust` package (version 5.4.6 Scrucca et al. 2016) for the model fitting and

computed the likelihoods, L , of each model. Model selection is based on the Bayesian information criterion (BIC Schwarz 1978): $\text{BIC} = 2 \ln L - k \ln N$, where k and N are the number of estimated parameters and the sample size respectively. We found that the optimal BIC requires three 2-dimensional Gaussian components to model our adopted data in $\gamma - c$ plane. In Figure 5, three different groups as clustered by GMM are represented by the symbols of different colour. According to their brightness concentration, we refer to these groups as "Sparse (S)", "Intermediate (I)" and "Dense (D)" hereafter. The corresponding labels of each GC are given in Table 2. Under this classification scheme, S group consists of purely Non-CCed GCs and D group only comprises CCed GCs. For the I group, there is a mixture of both Non-CCed and CCed GCs.

These three groups in $\gamma - c$ plane are well separated without much overlap (Figure 5). The averaged isolated pulsars fractions (f_s) in S, I and D groups are 0.64, 0.24 and 0.14, respectively, which increase progressively. These suggest such alternative classification is not unreasonable. And this prompts us to re-examine the possible differences of pulsar properties among these three groups. The comparisons of their eCDFs of P_{rot} , P_b , $L_{1.4\text{GHz}}$ and L_x are shown in Figure 6. The corresponding p -values as inferred from the A-D test are summarized in Table 3.

In comparing P_{rot} between S group and D group, we found that the pulsars in D groups generally rotate slower than those in S group. And such a difference is statistically significant ($p = 7 \times 10^{-3}$). Also, the distribution of $L_{1.4\text{GHz}}$ of S group is found to be significantly different from that of D group ($p = 0.013$) with the pulsars of D group significantly more luminous in L-band than those of S group. These results are fully consistent with those inferred from the comparison between Non-CCed and CCed populations as presented in Section 3.1 (cf. Figure 1 and Table 1).

For I group, which consists of both Non-CCed and CCed GCs, it is obvious that the P_{rot} distribution of I group is very similar to S group (see Figure 6). Examining the composition of this group, we found that $\sim 90\%$ of the pulsars in I group are originated from Non-CCed GCs which are dominated by the populations in 47 Tuc and Terzan 5. This might apparently account for the similarity. Nevertheless, despite the fact that the sample for $L_{1.4\text{GHz}}$ in I group is also dominated by Non-CCed pulsars which have a contribution of 83%, its distribution is comparable to that of D group.

We would like to point out that the selection effect on the sample

Name	N_b	N_s	r_c (pc)	$\log \rho_c$ ($L_\odot \text{pc}^{-3}$)	γ ($\gamma M4$)	Class
Non-core-collapsed GCs						
47 Tuc	19	10	0.36	4.88	6.57	I
M 10	2	0	0.77	3.54	0.67	S
M 12	2	0	0.79	3.23	0.42	S
M 13	4	2	0.62	3.55	0.52	S
M 14	5	0	0.79	3.36	0.25	S
M 2	6	0	0.32	4.00	1.05	I
M 22	2	2	1.33	3.63	0.59	S
M 28	10	4	0.24	4.86	7.88	I
M 3	6	0	0.37	3.57	0.62	I
M 4	1	0	1.16	3.64	1.00	I
M 5	6	1	0.44	3.88	1.02	I
M 53	4	1	0.35	3.07	0.21	S
M 71	5	0	0.63	2.83	0.40	S
M 92	1	0	0.26	4.30	2.53	I
NGC 1851	9	6	0.09	5.09	12.44	I
NGC 5986	1	0	0.47	3.41	0.40	S
NGC 6440	4	4	0.14	5.24	13.53	I
NGC 6441	3	6	0.13	5.26	10.93	I
NGC 6517	3	14	0.06	5.29	26.82	I
NGC 6539	1	0	0.38	4.15	1.55	I
NGC 6652	2	0	0.1	4.48	6.71	I
NGC 6712	1	0	0.76	3.18	0.29	S
NGC 6749	2	0	0.62	3.30	0.35	S
NGC 6760	1	1	0.34	3.89	1.35	I
Omega Cen	8	10	2.37	3.15	0.12	S
Terzan 5	24	20	0.16	5.14	13.00	I
Core-collapsed GCs						
M 15	1	8	0.14	5.05	8.89	D
M 30	2	0	0.06	5.01	25.42	D
M 62	9	0	0.22	5.16	9.82	I
NGC 362	5	1	0.18	4.74	5.85	I
NGC 6342	1	1	0.05	4.97	27.76	D
NGC 6397	2	0	0.05	5.76	254.79	D
NGC 6522	0	6	0.05	5.48	55.13	D
NGC 6544	3	0	0.05	6.06	275.92	I
NGC 6624	2	10	0.06	5.30	36.40	D
NGC 6752	1	8	0.17	5.04	18.81	D
Terzan 1	0	7	0.04	3.85	12.13	D

* **Note** : Number of binary pulsars N_b and isolated pulsars N_s from Manchester et al. (2005). Core radius r_c and central luminosity density, ρ_c from Harris (1996, 2010 edition). Disruption rates $\gamma \propto \rho_c^{0.5} r_c^{-1}$ from Eq. 2 in Verbunt & Freire (2014a), which are normalized with the value of M4. The class labels in the seventh column represent the groups of Sparse (S), Intermediate (I), and Dense (D) as determined by GMM (See Sec. 3.2).

Table 2. Updated statistics of single and binary pulsars as well as the structural parameters of GCs.

of $L_{1.4\text{GHz}}$ might prevent us from drawing any firm conclusion in comparing this property among these three groups. While the sample size for P_{rot} is 279, there are only 59 pulsars that have their measures of $L_{1.4\text{GHz}}$ available for analysis. This effect is particularly obvious in I group which has its sample size reduced from 179 for P_{rot} to 29 for $L_{1.4\text{GHz}}$. This can be accounted for by the fact that only those sufficiently bright pulsars can have their radio fluxes reliably measured. It is uncertain whether the $L_{1.4\text{GHz}}$ distribution of I group will remain comparable D group when the fainter pulsars are included. Pulsar surveys with improved sensitivity might help to resolve this issue in the future.

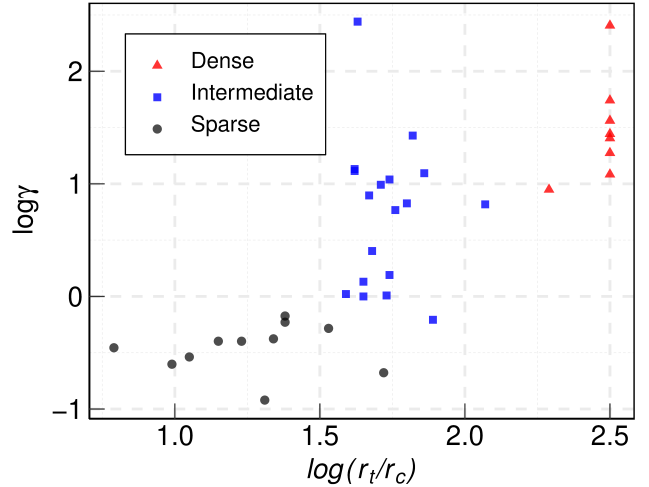


Figure 5. Unsupervised classification of GCs in a plane spanned by the disruption rate γ and the central concentration parameter c with the method of 2-dimensional Gaussian Mixture Model (GMM).

	S vs D	S vs I	D vs I
P_{rot}	0.007	0.898	0.0002
P_b	0.612	0.214	0.472
$L_{1.4\text{GHz}}$	0.013	0.012	0.902
L_x	0.844	0.522	0.406

Table 3. Null hypothesis probabilities of A-D test for comparing P_{rot} , P_b , $L_{1.4\text{GHz}}$ and L_x among S, I and D groups as classified by GMM.

4 SUMMARY & DISCUSSION

Motivated by the recent work by Lee et al. (2023) which has identified the differences in various properties between the GC and GF pulsar populations, we proceed to investigate whether the variation of intracluster dynamics between CCed and Non-CCed GCs can further diversify the pulsar properties (see Figure 1 and Figure 2).

We found that pulsars in CCed GCs generally rotate slower than those in Non-CCed GCs. This is consistent with the notion that secondary encounters in CCed GCs are enhanced (Verbunt & Freire 2014a), which presumably results in the prevalence of isolated MSPs and fewer X-ray binaries than in Non-CCed GCs with comparable primary encounter rates (Bahramian et al. 2013; Verbunt & Freire 2014a; Kremer et al. 2022). The increased binary disruption efficiency in CCed GCs likely interrupts the angular momentum transfer at an earlier stage of recycling. Consequently, the slower rotation of pulsars in CCed GCs is not unexpected (see also Ivanova et al. 2008).

If the recycling process is halted at an earlier epoch, not only a slower rotating pulsar result, but we should also expect a stronger surface magnetic field than their counterparts in Non-CCed GCs because the magnetic decay due to the mass transfer is suppressed (see the discussion in Lee et al. 2023). For pulsars, the strength of the dipolar surface magnetic field can be estimated by their rotational period P_{rot} and the corresponding spin-down rate \dot{P}_{rot} namely $B_s \approx \sqrt{\frac{3c^2 I}{2\pi^2 R_{NS}^6} \dot{P}_{\text{rot}} P_{\text{rot}}}$, where c is the speed of light and R_{NS} is the radius of the neutron star. However, such estimation for the pulsars in GCs is complicated by the accelerations in the gravitational potential of a GC, which can bias the measurement of \dot{P}_{rot} . Up to now, there are only a handful of GC pulsars with their intrinsic \dot{P}_{rot} estimated

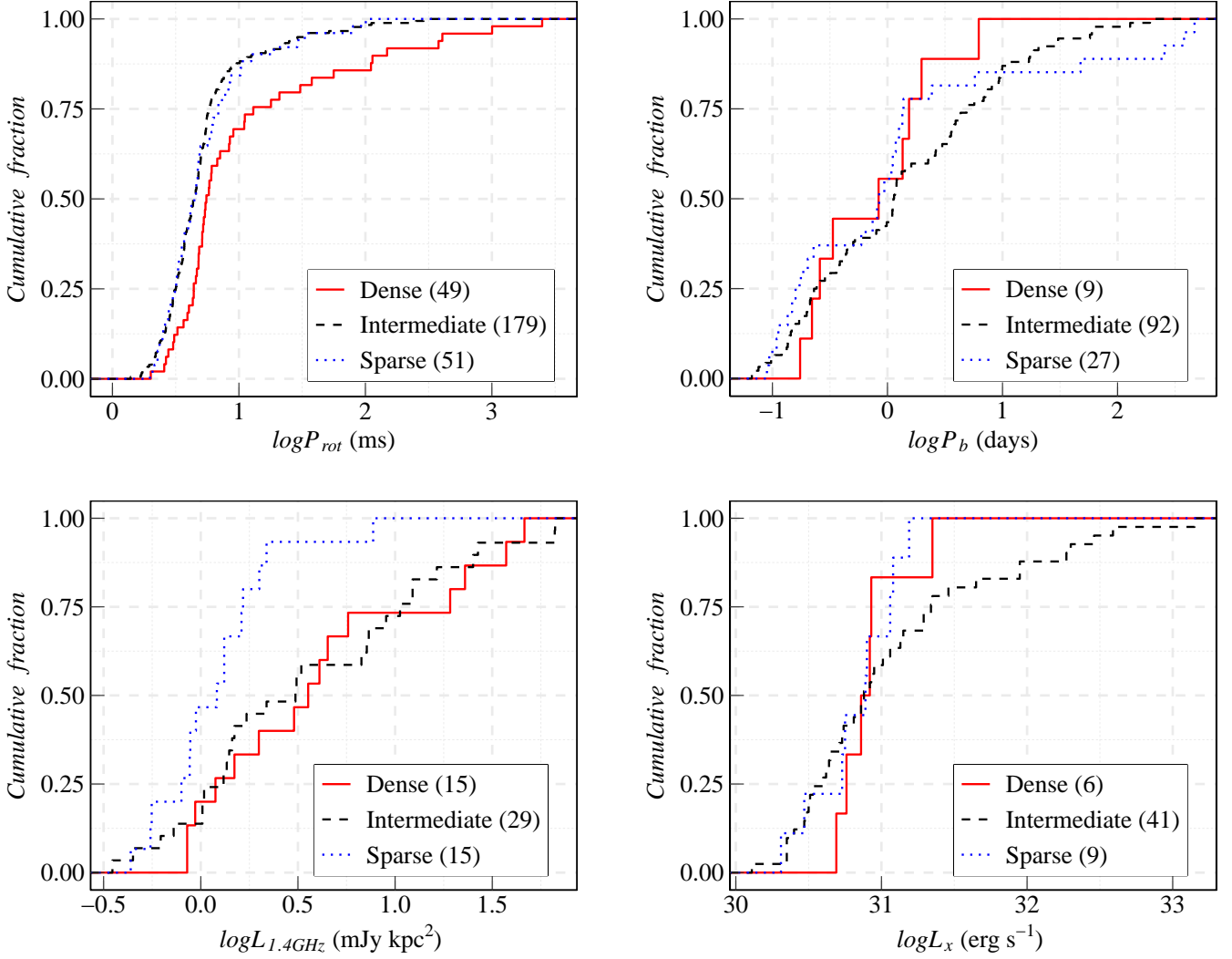


Figure 6. Comparisons of eCDFs of the selected pulsar properties among S, I and D groups as determined by GMM. The bracketed numbers in the legends show the corresponding sample sizes.

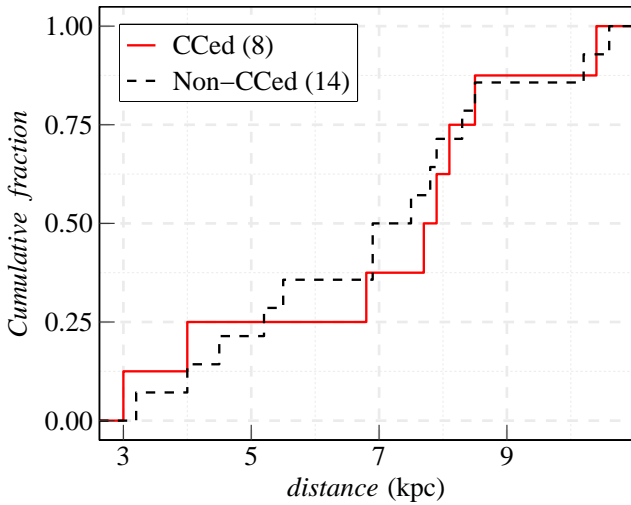


Figure 7. Comparison of eCDFs of the distance between CCed GCs and Non-CCed GCs in our sample.

(cf. Tab. 4 in Lee et al. 2023) and therefore, we are not able to directly compare the B_s of the pulsars in CCed and Non-CCed GCs.

On the other hand, as a pulsar radiates by tapping its rotational energy, the radiation power should be proportional to the spin-down power \dot{E} which is expressed as $\dot{E} = 4\pi^2 I \dot{P}_{\text{rot}} P_{\text{rot}}^{-3} \propto B_s^2 P_{\text{rot}}^{-4}$ where I is the moment of inertia. Therefore, the radio luminosity $L_{1.4\text{GHz}}$ can be treated as a proxy for probing B_s of the GC pulsars.

Our analysis indicates that $L_{1.4\text{GHz}}$ of the pulsars in CCed GCs are significantly higher than those in Non-CCed GCs (cf. Figure 1). Together with the fact that P_{rot} of CCed GC pulsars are longer than those in Non-CCed GCs, we can infer that B_s of CCed GC pulsars are stronger than those in Non-CCed GCs which is in line with our aforementioned speculation.

To investigate whether the difference in $L_{1.4\text{GHz}}$ is genuine, we have further checked whether such a difference can be a result of the observational effect. If a GC is close to us, a flux-limited survey will uncover more faint sources than those in the more distant GCs. For examining this issue, we compared the distances d between the CCed and Non-CCed GCs in our sample, and the results are shown in Figure 7. The medians of d of CCed and Non-CCed GCs are 6.8 kpc and 6.9 kpc respectively. With A-D test, we do not find any

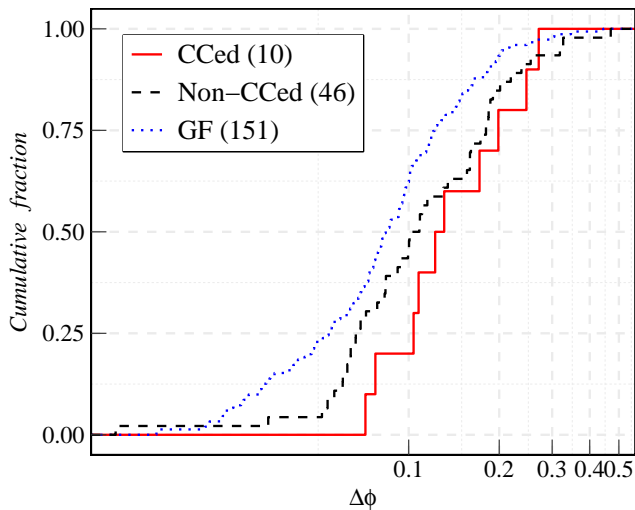


Figure 8. Comparison of eCDFs of the estimates of radio beam sizes $\Delta\phi$ of MSPs in CCed GCs, Non-CCed GCs, and the GF.

significant difference between these two eCDFs ($p > 0.05$). And hence, we conclude that the difference in $L_{1.4\text{GHz}}$ between CCed and Non-CCed GCs is genuine.

On the other hand, the A-D test indicates that the differences in $L_{1.4\text{GHz}}$ and L_x between the GF and GC MSP populations are statistically significant. However, we notice that many GF MSPs are located in our proximity. The medians of d for radio-selected MSPs in GCs and GF in our sample are found to be 6.9 kpc and 1.7 kpc, respectively. A-D test yields a p -value of $\sim 10^{-22}$ which indicates a very significant difference between their distributions of d . Consequently, the excess at the lower end of the distribution of $L_{1.4\text{GHz}}$ for GF MSPs (Figure 2) can be a result of observational bias. This bias also affects the comparison of L_x between MSPs in GCs (median $d = 4.9$ kpc) and GF (median $d = 1.2$ kpc) in our sample.

In conclusion, our results demonstrate that CCed and Non-CCed GC pulsar populations exhibit differences in their rotation rates and radio luminosities, with CCed GC pulsars rotating slower and having higher radio luminosities. This supports the idea that the recycling process is halted earlier in CCed GCs, leading to stronger surface magnetic fields and slower rotations.

For further examining the effect of dynamical effects on the structure of the surface magnetic field, we would like to compare the radio beam sizes of MSPs in GF, CCed GCs, and Non-CCed GCs. The beam sizes can be estimated by $\Delta\phi = W_{50}/P_{\text{rot}}$, where W_{50} is the pulse width at 50% of the peak in the unit of time as obtained from the ATNF catalog (Manchester et al. 2005). The comparisons of $\Delta\phi$ among three populations are given in Figure 8.

It is interesting to note that the $\Delta\phi$ of MSPs in GF is smaller than those in Non-CCed and CCed GCs. With A-D test, we find $\Delta\phi$ of the GF population is significantly smaller than those of Non-CCed MSPs (p -value ~ 0.01) and CCed MSPs (p -value ~ 0.02). We also note that the $\Delta\phi$ from Non-CCed GCs is apparently smaller than that from CCed GCs, although the A-D test does not yield a p -value below our pre-defined criterion.

These results conform with the expectation that different recycling histories can lead to different surface magnetic field structures. Chen & Ruderman (1993) argued that mass accretion could reduce the polar cap radius and hence the size of the open field line region. This notion is supported by Kramer et al. (1998), which found the

open angle of GF MSPs is smaller than that expected from the dipolar geometry (cf. Fig. 12 in their paper).

The fact that the $\Delta\phi$ of GF MSPs is smaller than those of GC MSPs is consistent with the scenario that the accretion phase of GC MSPs is shortened by dynamical disruption, as suggested by Lee et al. (2023). Since the disruption rate is generally higher in CCed GCs (see Table 2 & Figure 4), the MSPs in CCed GCs should have a larger beam size than those in Non-CCed GCs. However, a firm conclusion is precluded by the current sample size. With more samples available in the future, the comparison of $\Delta\phi$ between these two classes of GC MSPs should be revisited.

We have to point out a caveat in the comparison of $\Delta\phi$ presented here. First, owing to the complexity of the radio pulse profile, W_{50} should be considered as a poor estimator for the size of the emission beam. Second, beam size should be a function of observing frequency. However, such information is not available in the ATNF catalog. A more accurate determination of the emission geometry should be derived from fitting the polarization data. Therefore, we strongly encourage a dedicated study to compare the emission geometry of MSPs in GF and GCs with radio polarization, which can help to scrutinize our hypothesis.

Lastly, we would like to emphasize that all the aforementioned discussions are based on the conventional CCed/Non-CCed classification of GCs, which relies on photometric measurements (Trager et al. 1995; Harris 1996). In Section 3.2, we have pointed out a possible ambiguity of this conventional classification scheme. Bianchini et al. (2018) have also mentioned that there is no robust connection between the photometric central concentration and the dynamical state of a GC.

By combining the central concentration parameter c and a dynamical measure of disruption rate γ , we have shown that the GCs in our sample can be divided into three groups (Figure 5). For two groups maximally separated in the $\gamma - c$ plane, namely S group and D group, they purely comprised Non-CCed GCs and CCed GCs, respectively (cf. Table 2). By comparing the distributions of P_{rot} and $L_{1.4\text{GHz}}$ between these two groups, the differences remain to be statistically significant. On the other hand, the intermediate I group has a mixture of CCed and Non-CCed GCs. Both flux-limited samples and a strong bias in I group by the pulsars from a few Non-CCed GCs (e.g. 47 Tuc and Terzan 5) preclude any conclusive comparison with the other two groups.

This has also raised a concern that the classification scheme of GCs might not be unique. In view of the complex evolution of GCs (e.g. Ivanova et al. 2006; Hong et al. 2017), the description of both dynamical status and structure of GCs can be more complicated than the binary classification as simple as CCed or Non-CCed. For example, by examining the radial distribution of blue stragglers, Ferraro et al. (2012) have shown that the dynamical age of GCs can be divided into three groups. With a more comprehensive classification scheme proposed by further studies, the differences in pulsar properties among different groupings can be reexamined.

ACKNOWLEDGEMENTS

K.O is supported by the National Research Foundation of Korea grant 2022R1F1A1073952 and 2022R1A6A3A13071461. C.Y.H. is supported by the research fund of Chungnam National University and by the National Research Foundation of Korea grant 2022R1F1A1073952. J.T. is supported by the National Key Research and Development Program of China (grant No. 2020YFC2201400) and the National Natural Science Foundation of China (NSFC, grant No. 12173014). A.K.H.K. is supported by the National Science and Technology Council of Taiwan through grant 111-2112-M-007-020.

P.H.T. is supported by NSFC grant No. 12273122 and the China Manned Space Project (No. CMS-CSST-2021-B09). K.L.L. is supported by the National Science and Technology Council of the Republic of China (Taiwan) through grant 111-2636-M-006-024, and he is also a Yushan Young Fellow supported by the Ministry of Education of the Republic of China (Taiwan).

Ye C. S., Kremer K., Rodriguez C. L., Rui N. Z., Weatherford N. C., Chatterjee S., Fragione G., Rasio F. A., 2022, *ApJ*, 931, 84

This paper has been typeset from a $\text{\TeX}/\text{\LaTeX}$ file prepared by the author.

DATA AVAILABILITY

The data underlying this article were accessed from Chandra Data Archive (<https://cda.harvard.edu/chaser/>) and ATNF (<https://www.atnf.csiro.au/research/pulsar/psrcat/>).

REFERENCES

- Alpar M. A., Cheng A. F., Ruderman M. A., Shaham J., 1982, *Nature*, 300, 728
- Bahramian A., Heinke C. O., Sivakoff G. R., Gladstone J. C., 2013, *The Astrophysical Journal*, 766, 136
- Bianchini P., Webb J. J., Sills A., Vesperini E., 2018, *MNRAS*, 475, L96
- Chen K., Ruderman M., 1993, *ApJ*, 408, 179
- Clark G. W., 1975, *ApJ*, 199, L143
- Cumming A., Arras P., Zweibel E., 2004, *ApJ*, 609, 999
- Fabian A. C., Pringle J. E., Rees M. J., 1975, *MNRAS*, 172, 15
- Fabian A. C., Pringle J. E., Verbunt F., Wade R. A., 1983, *Nature*, 301, 222
- Ferraro F. R., et al., 2012, *Nature*, 492, 393–395
- Fregeau J. M., Rasio F. A., 2007, *ApJ*, 658, 1047
- Gelman A., Carlin J., Stern H., Dunson D., Vehtari A., Rubin D., 2013, *Bayesian Data Analysis*, Third Edition. Chapman & Hall/CRC Texts in Statistical Science, Taylor & Francis, <https://books.google.co.kr/books?id=ZXL6AQAQBAJ>
- Harris W. E., 1996, *AJ*, 112, 1487
- Hong J., Vesperini E., Belloni D., Giersz M., 2017, *MNRAS*, 464, 2511
- Hui C. Y., Li K. L., 2019, *Galaxies*, 7, 93
- Hui C. Y., Cheng K. S., Taam R. E., 2010, *ApJ*, 714, 1149
- Ivanova N., Heinke C. O., Rasio F. A., Taam R. E., Belczynski K., Fregeau J., 2006, *Monthly Notices of the Royal Astronomical Society*, 372, 1043
- Ivanova N., Heinke C. O., Rasio F. A., Belczynski K., Fregeau J. M., 2008, *Monthly Notices of the Royal Astronomical Society*, 386, 553
- Katz J. I., 1975, *Nature*, 253, 698
- King I. R., 1966, *AJ*, 71, 64
- Kramer M., Xilouris K. M., Lorimer D. R., Doroshenko O., Jessner A., Wielebinski R., Wolszczan A., Camilo F., 1998, *ApJ*, 501, 270
- Kremer K., Ye C. S., Kiroğlu F., Lombardi J. C., Ransom S. M., Rasio F. A., 2022, *The Astrophysical Journal Letters*, 934, L1
- Lee H. M., Ostriker J. P., 1986, *ApJ*, 310, 176
- Lee J., Hui C. Y., Takata J., Kong A. K. H., Tam P.-H. T., Li K.-L., Cheng K. S., 2023, *The Astrophysical Journal*, 944, 225
- Lombardi J. C. J., Proulx Z. F., Dooley K. L., Theriault E. M., Ivanova N., Rasio F. A., 2006, *ApJ*, 640, 441
- Lynden-Bell D., Wood R., 1968, *MNRAS*, 138, 495
- Manchester R. N., Hobbs G. B., Teoh A., Hobbs M., 2005, *AJ*, 129, 1993
- Manning C. D., Raghavan P., Schütze H., 2008, *Introduction to Information Retrieval*. Cambridge University Press, Cambridge, UK, <http://nlp.stanford.edu/IR-book/information-retrieval-book.html>
- Pooley D., et al., 2003, *ApJ*, 591, L131
- Press W. H., Teukolsky S. A., 1977, *ApJ*, 213, 183
- Radhakrishnan V., Srinivasan G., 1982, *Current Science*, 51, 1096
- Rivera Sandoval L. E., et al., 2018, *MNRAS*, 475, 4841
- Schwarz G., 1978, *The Annals of Statistics*, 6, 461
- Scrucca L., Fop M., Murphy T. B., Raftery A. E., 2016, *The R Journal*, 8, 289
- Sigurdsson S., Phinney E. S., 1995, *ApJS*, 99, 609
- Trager S. C., King I. R., Djorgovski S., 1995, *AJ*, 109, 218
- Verbunt F., Freire P. C. C., 2014a, *A&A*, 561, A11
- Verbunt F., Freire P. C. C., 2014b, *A&A*, 561, A11
- Ye C. S., Kremer K., Chatterjee S., Rodriguez C. L., Rasio F. A., 2019, *ApJ*, 877, 122